

EARLY CAREER SCHOLARS IN MATERIALS SCIENCE

Thermodynamic properties of rare-earth alloys by electrochemical emf measurements

Timothy Lichtenstein , Sanghyeok Im, Chen-Ta Yu, Hojong Kim^{a)} 

Materials Science and Engineering, The Pennsylvania State University, University Park, Pennsylvania 16802, USA

^{a)}Address all correspondence to this author. e-mail: huk29@psu.edu

Received: 26 May 2020; accepted: 27 July 2020; published online: 4 February 2021

Thermodynamic properties of Nd–Bi and Nd–Sn alloys were determined *via* electromotive force (emf) measurements at 725–1075 K. The emf measurements of an Nd–Bi alloy at mole fraction $x_{\text{Nd}} = 0.20$ were conducted using a solid $\text{CaF}_2\text{--NdF}_3$ electrolyte relative to pure Nd(s). The emf values from the $\text{CaF}_2\text{--NdF}_3$ electrolyte were verified in separate experiments in molten LiCl--KCl--NdCl_3 where pure Nd(s) was electrodeposited. The Nd–Bi ($x_{\text{Nd}} = 0.20$) exhibited two-phase behavior with a peritectic reaction ($\text{L} + \text{NdBi} = \text{NdBi}_2$) at 926 K from differential scanning calorimetry. The two-phase Nd–Bi ($x_{\text{Nd}} = 0.20$) was employed as a stable reference electrode in molten LiCl--KCl--NdCl_3 for emf measurements of Nd–Bi ($x_{\text{Nd}} = 0.15\text{--}0.40$) and Nd–Sn ($x_{\text{Nd}} = 0.10$) alloys. The emf measurements of these alloys were reproducible during thermal cycles over 50 h and were used to calculate thermodynamic properties, including the partial molar Gibbs energy, entropy, and enthalpy.



Dr. Hojong Kim received his B.S. in Materials Science and Engineering from Seoul National University in South Korea in 2000. He went on to earn his Ph.D. degree at MIT in 2004. His doctoral research sought to identify the corrosion mechanisms of constructional alloys in high-temperature and high-pressure steam environments in the Uhlig Corrosion Laboratory. After graduate research, Dr. Kim worked as a senior research engineer at Samsung-Corning Precision Glass to improve the process yield for thin-film-transistor liquid-crystal display (TFT-LCD) glass manufacturing by engineering high-temperature refractory materials. After 5 years of industrial experience, Dr. Kim returned to MIT as a post-doctoral researcher to contribute to the growing need for sustainable technology, with a research focus on molten oxide electrolysis for carbon-free iron production and liquid metal batteries for large-scale energy storage. Dr. Kim joined the Penn State Material Science and Engineering in 2014 as an assistant professor. His current research focuses on separation of energy-critical materials and development of corrosion-resistant alloys. He is the recipient of the 2019 NSF-CAREER award and 2015 doctoral new investigator award from American Chemical Society. He served as the chair (2017–2019) and vice-chair (2015–2017) of hydrometallurgy and electrometallurgy committee at TMS.

Introduction

Thermodynamic properties of rare-earth elements are essential for developing efficient rare-earth recovery processes from primary and/or secondary resources to enable a sustainable materials cycle and deploy clean energy technologies such as electric vehicles and wind turbines that rely on permanent magnets (NdFeB) [1, 2, 3]. This work investigated thermodynamic properties of binary Nd–Bi and Nd–Sn alloys by electromotive force (emf) measurements which directly determine the chemical potential of Nd *via* the Nernst equation. Using molten halide salts or solid electrolytes such as CaF_2 and β -alumina,

thermochemical properties of alkali and alkaline-earth alloys were determined *via* accurate emf measurements, including Li–Bi, Na–Bi, Ca–Bi, Ba–Bi, and Sr–Bi [4, 5, 6, 7, 8, 9]. However, reliable emf measurements of rare-earth alloys have been a challenge due to the multivalent states (Nd^{3+} and Nd^{2+}) that result in a side reaction between pure Nd and the electrolyte by disproportionation ($\text{Nd} + 2\text{NdCl}_3 \rightarrow 3\text{NdCl}_2$), leading to a loss of Nd into molten salt electrolytes [10, 11, 12, 13].

The emf measurements of Nd alloys were investigated using the molten LiCl--KCl--NdCl_3 electrolyte by Lebedev et al. for Nd–Bi alloy with [liquid (L) + NdBi_2] phases at

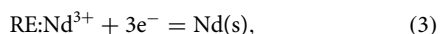
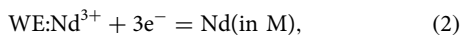
673–973 K and by Kulagina and Bayanov for Nd–Sn alloys at mole fractions $x_{\text{Nd}} = 0.006\text{--}0.28$ at 773, 873, and 973 K [14, 15, 16]. Unfortunately, these prior works provide little detail on the stability of the pure Nd(s) electrode, thus the reliability of the measured thermodynamic properties. This work measured the emf values of the Nd–Bi and Nd–Sn alloys at 725–1250 K in molten salt electrolytes (LiCl–KCl–NdCl₃ and LiF–CaF₂–NdF₃) and evaluated the stability and reproducibility of the measurements using pure Nd(s) as the reference system to identify suitable methodologies that mitigate the side reaction for reliable emf measurements.

This work employed a new solid CaF₂–NdF₃ (97–3 mol%) electrolyte for emf measurements of an Nd–Bi alloy ($x_{\text{Nd}} = 0.20$) since the Nd³⁺ ions were shown to involve a single reduction step (Nd³⁺ + 3e[−] = Nd) in fluoride electrolyte (LiF–CaF₂) [17], and the solid CaF₂-based electrolytes enabled accurate emf measurements of reactive alkaline-earth alloys [9, 18, 19, 20]. The emf values from the solid electrolyte were compared to the results from a transient technique in the molten LiCl–KCl–NdCl₃ electrolyte where pure Nd(s) is electrodeposited in small quantities. In addition, a two-phase Nd–Bi ($x_{\text{Nd}} = 0.20$) alloy was utilized as a less-reactive reference electrode material in the molten LiCl–KCl–NdCl₃ electrolyte. The effect of these new methodologies was evaluated by comparing the emf results of Nd–Bi and Nd–Sn alloys during thermal cycles between 725 and 1075 K.

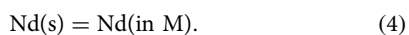
The thermodynamic properties of binary Nd–M alloys (M = Bi or Sn) were determined by emf measurements of these alloys relative to pure Nd metal using the following electrochemical cell:



where pure Nd(s) is the reference electrode (RE), Nd–M alloy is the working electrode (WE), and the metal M is electrochemically more noble than Nd. The half-reactions for this cell are



and the overall cell reaction is



For the overall reaction, the change in partial molar Gibbs energy of Nd ($\Delta\bar{G}_{\text{Nd}}$) is given by

$$\Delta\bar{G}_{\text{Nd}} = \bar{G}_{\text{Nd(in M)}} - G_{\text{Nd}}^0 = RT \ln a_{\text{Nd}}, \quad (5)$$

where $\bar{G}_{\text{Nd(in M)}}$ is the chemical potential of Nd in metal M, G_{Nd}^0 is the standard chemical potential of pure Nd(s), a_{Nd} is the activity of Nd, R is the universal gas constant, and T is the temperature in Kelvin. The emf of this cell (E) is directly related to

$\Delta\bar{G}_{\text{Nd}}$ by the Nernst equation:

$$E = -\frac{\Delta\bar{G}_{\text{Nd}}}{3F} = -\frac{RT}{3F} \ln a_{\text{Nd}}, \quad (6)$$

where F is the Faraday constant.

Results and Discussion

Emf measurements of Nd–Bi alloy in molten salts

The emf values of the Nd–Bi ($x_{\text{Nd}} = 0.20$) alloy were measured relative to pure Nd(s) in LiCl–KCl–NdCl₃ at 700–1000 K and LiF–CaF₂–NdF₃ at 1050–1250 K (Fig. 1). In LiCl–KCl–NdCl₃, the emf measurement was initially stable at ~0.76 V and 700 K; however, a sudden decrease in emf was observed sporadically during the first heating cycle, and the emf decreased to near zero during the cooling cycle [Fig. 1(a)]. A more stable emf measurement was achieved in LiF–CaF₂–NdF₃ even at a higher temperature; however, the emf values were not reproduced during the following cooling cycle and continuously decreased [Fig. 1(b)].

Based on a set of stable emf values during the first heating cycle [Fig. 1(c)], it is clear that the uncertainty in emf values at a given temperature can be as large as 36 mV and tend to grow at higher temperatures and/or later measurements. The observation indicates a side reaction between Nd(s) and molten salts, generating unreliable emf values. Lebedev et al. reported the emf versus T of the Nd–Bi alloy with [L + NdBi₂] phases at 673–973 K [14, 16], using a similar approach with pure Nd (s) in the LiCl–KCl–NdCl₃ electrolyte. Lebedev et al. also observed that emf values continuously decrease as temperature increases [Fig. 1(c)], but the results did not agree with this work except for the initial value at 700 K.

Differential scanning calorimetry (DSC) measurements of the Nd–Bi ($x_{\text{Nd}} = 0.20$) detected three characteristic transition reactions during heating cycle (Fig. 2). The eutectic [I: L = Bi + NdBi₂ (or Nd₃Bi₇) at 536 K] and peritectic [III: L + NdBi = NdBi₂ at 926 K] reactions are in agreement with the binary Nd–Bi phase diagram [21]; the reaction (II) is thought to be a peritectic reaction [II: L + NdBi₂ = Nd₃Bi₇ at 771 K] based upon the recent finding of the Nd₃Bi₇ compound by Ovchinnikov et al. [22]. The peritectic reactions at 771 and 926 K are first-order transitions ($d\Delta\bar{G}_{\text{Nd}}/dT$) which would result in a discontinuity in the slope (dE/dT); however, neither results from this work nor Lebedev et al. could observe these transitions, possibly due to a large uncertainty in emf measurements using pure Nd(s) in molten salts [Fig. 1(c)].

Emf measurements of Nd–Bi alloy in solid CaF₂–NdF₃ electrolyte

For more reliable emf measurements of Nd–Bi ($x_{\text{Nd}} = 0.20$), this work employed two additional approaches in efforts to

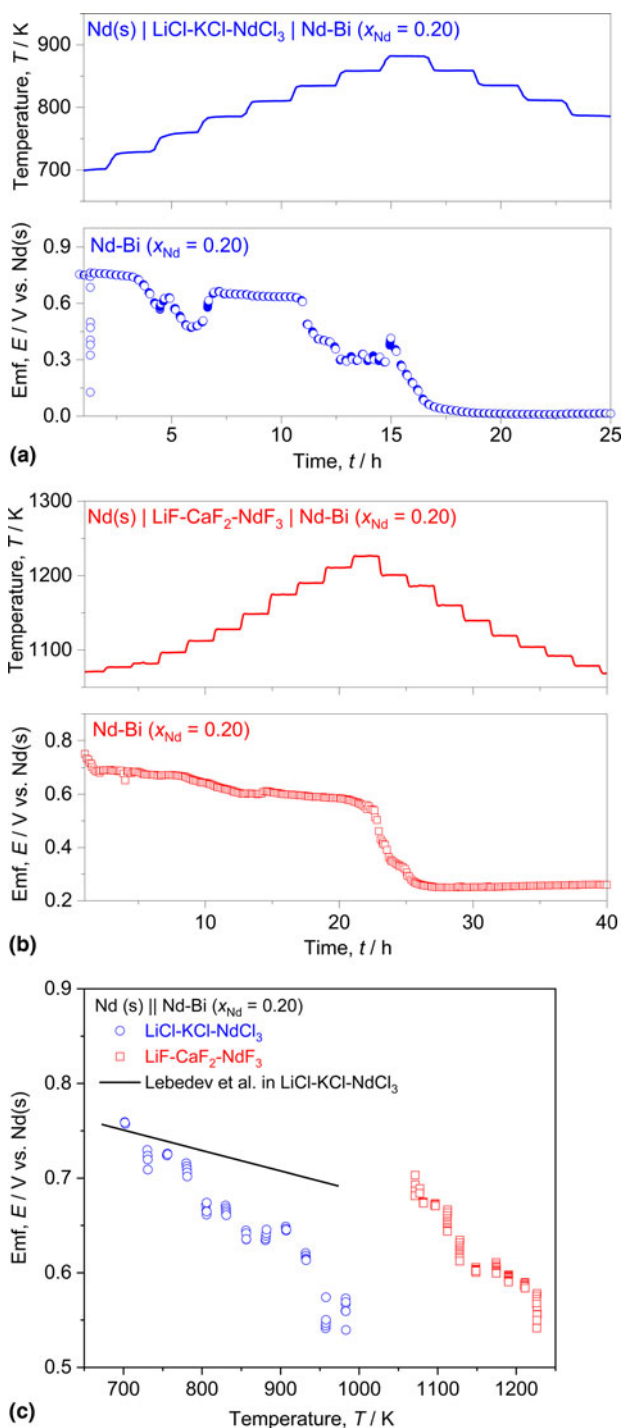


Figure 1: Emf measurements of Nd-Bi ($x_{Nd} = 0.20$) during the thermal cycle using pure Nd metal as the RE in molten salt electrolytes: (a) LiCl-KCl-NdCl₃, (b) LiF-CaF₂-NdF₃, and (c) emf as a function of temperature, compared to the result by Lebedev et al. at 673–973 K [14, 16].

mitigate side reactions between Nd(s) and molten salts. First, a solid CaF₂-NdF₃ (97–3 mol%) served as the electrolyte in place of molten salts, Nd(s) | CaF₂-NdF₃(s) | Nd-Bi ($x_{Nd} = 0.20$), taking advantage of slow reaction/transport kinetics between the two solid phases of pure Nd and CaF₂-NdF₃. Second, a

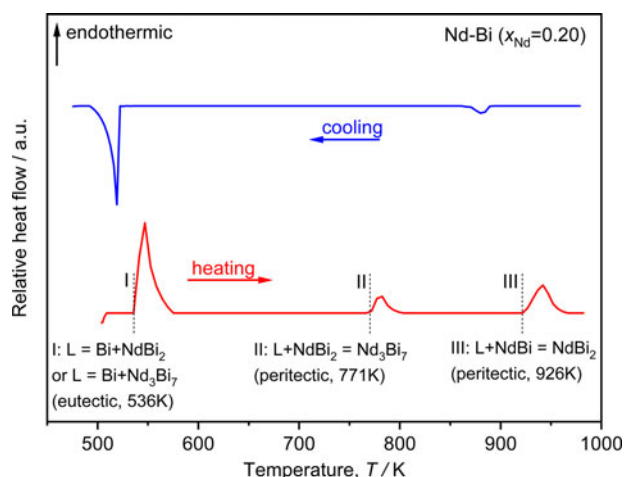


Figure 2: DSC measurement of Nd-Bi ($x_{Nd} = 0.20$) at 20 K/min during heating and cooling cycles.

three-electrode cell in molten LiCl-KCl-NdCl₃ was used for a transient technique where pure Nd is electrodeposited onto an inert tungsten WE, followed by open-circuit potential (OCP) measurement relative to the Nd-Bi ($x_{Nd} = 0.20$) RE.

Solid CaF₂-NdF₃ electrolyte

The emf cell, Nd(s) | CaF₂-NdF₃(s) | Nd-Bi ($x_{Nd} = 0.20$), was initially heated to the highest temperature at 1025 K to establish electrical contact with the Nd-Bi alloy, then cooled in 25 K increments [Fig. 3(a)]. Compared to the measurements in molten salts, the emf measurements were stable during the first cooling cycle and were partially reproducible during the following heating cycle with ~20 h cell lifetime. The temperature-dependent emf data exhibit a discontinuity in the slope (dE/dT) at ~913 K [Fig. 3(b)], indicating a peritectic transition [III: L + NdBi = NdBi₂] according to the DSC measurement (Fig. 2). Furthermore, the emf measurements in solid electrolyte were accurate within ~22 mV range between 0.71 and 0.74 V [Fig. 3(b)], compared to ~220 mV range between 0.54 and 0.76 V in molten salts [Fig. 1(c)].

Transient technique in molten LiCl-KCl-NdCl₃

A constant cathodic current of 0.2 A was applied for 5 s (1 C) for electrodeposition of Nd (0.50 mg) at the tungsten WE, followed by OCP measurements for 120 s (Fig. 4). At 857 K, the OCP of the pure Nd versus Nd-Bi ($x_{Nd} = 0.20$) was stable for ~40 s, but became unstable due to the side reaction with the electrolyte. The emf value at each temperature was taken near the end of the stable OCP measurement, consistently at the inflection point. The emf values from the transient technique were in agreement with the results from the solid CaF₂-NdF₃ electrolyte [Fig. 3(b)].

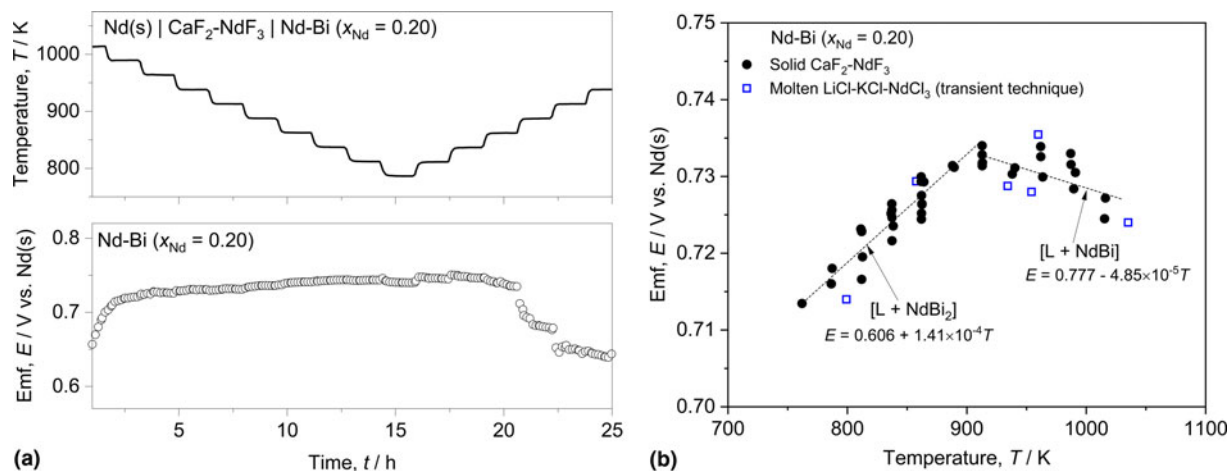
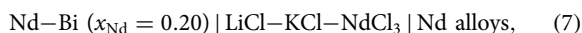


Figure 3: (a) Emf measurements of Nd–Bi ($x_{\text{Nd}} = 0.20$) during the thermal cycle using pure Nd metal as the RE in solid $\text{CaF}_2\text{-NdF}_3$ electrolyte and (b) emf as a function of temperature, where the dashed lines represent a linear fit.

Emf measurements of Nd alloys with two-phase alloy RE

In binary Nd alloys in equilibrium, the activity of Nd remains invariant with composition in a two-phase region at a given temperature, resulting in a constant emf value [Eq. (6)]. This unique two-phase behavior has been widely observed in a number of alloy systems [4, 5, 6, 7, 8, 9] and is often used as a stable, less-reactive RE [23, 24, 25, 26]. Similarly, this work conducted emf measurements of selected Nd alloys in the LiCl–KCl–NdCl₃ electrolyte:



where the two-phase Nd–Bi ($x_{\text{Nd}} = 0.20$) served as the RE, and Nd alloys of Nd–Bi and Nd–Sn as the WE.

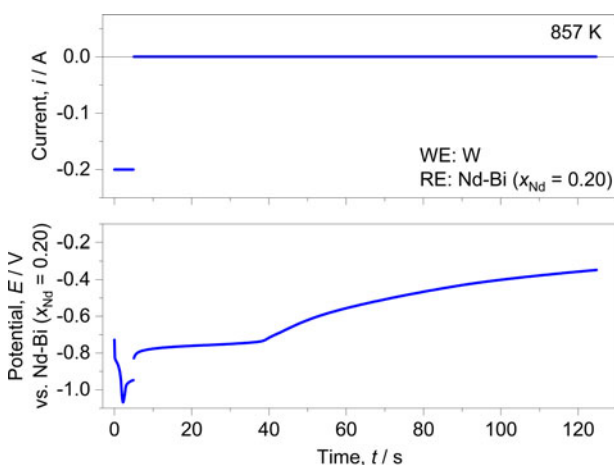


Figure 4: Transient technique for emf measurements of Nd–Bi ($x_{\text{Nd}} = 0.20$) in the molten LiCl–KCl–NdCl₃ electrolyte at 857 K: electrodeposition of pure Nd on W electrode, followed by OCP measurement between Nd and Nd–Bi ($x_{\text{Nd}} = 0.20$).

Nd–Bi alloys

The potential difference between two identical Nd–Bi ($x_{\text{Nd}} = 0.20$) alloys was maintained at less than ± 5 mV during the entire measurement (>40 h) without an indication of cell degradation [Fig. 5(a)]. The emf measurement between Nd–Bi ($x_{\text{Nd}} = 0.40$) and Nd–Bi ($x_{\text{Nd}} = 0.20$) was highly stable and reproducible, seen from the symmetric profile of both emf and temperature. Using the results in Fig. 3(b), the emf of Nd–Bi alloys ($x_{\text{Nd}} = 0.15\text{--}0.40$) were plotted relative to pure Nd(s) as a function of temperature [Fig. 5(b)].

At 926–1076 K, the emf trajectory of Nd–Bi ($x_{\text{Nd}} = 0.40$) was nearly identical to that of Nd–Bi ($x_{\text{Nd}} = 0.20$) due to the identical two-phase [L + NdBi] behavior but was more negative than Nd–Bi ($x_{\text{Nd}} = 0.20$) at 774–926 K due to the [NdBi₂ + NdBi] phase behavior different from [L + NdBi₂] for Nd–Bi ($x_{\text{Nd}} = 0.20$) [Fig. 5(b)]. The emf trajectories of Nd–Bi alloys at $x_{\text{Nd}} = 0.15\text{--}0.30$ were nearly identical due to the same phase behavior at 750–1050 K.

Nd–Sn alloys

The emf measurement of Nd–Sn ($x_{\text{Nd}} = 0.10$) using Nd–Bi ($x_{\text{Nd}} = 0.20$) RE was stable and reproducible during the thermal cycle [Fig. 6(a)]. When the emf values versus pure Nd(s) were plotted as a function of temperature over 724–1079 K [Fig. 6(b)], a linear emf–*T* relation was observed where two phases of [L + NdSn₃] are stable for $x_{\text{Nd}} = 0.10$ [27]. Kulagina and Bayanov reported the emf values of the Nd–Sn ($x_{\text{Nd}} = 0.10$) at 773–973 K [Fig. 6(b)] using an emf measurement cell: Nd(s) | LiCl–KCl–NdCl₃ | Nd–Sn [15]. Interestingly, the temperature dependence of the emf is contrary to this work, while the range of emf values is about the same. The use of pure Nd(s) in molten LiCl–KCl–NdCl₃ is thought to result in a side reaction

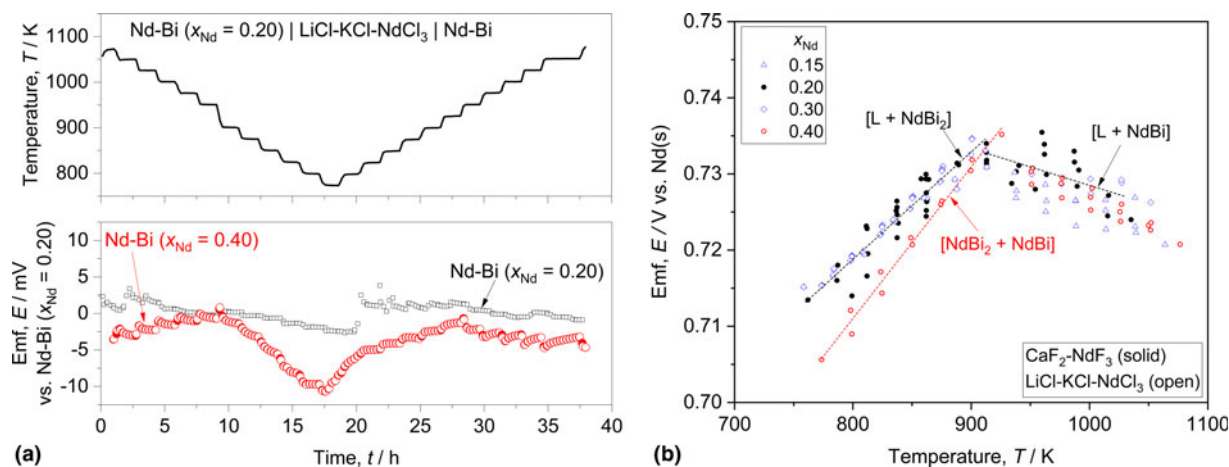


Figure 5: (a) Emf measurements of Nd-Bi ($x_{Nd} = 0.40$) during the thermal cycle using Nd-Bi ($x_{Nd} = 0.20$) as the RE in the molten LiCl-KCl-NdCl₃ electrolyte and (b) emf as a function of temperature for various Nd-Bi alloys ($x_{Nd} = 0.15-0.40$), where the dashed lines represent a linear fit.

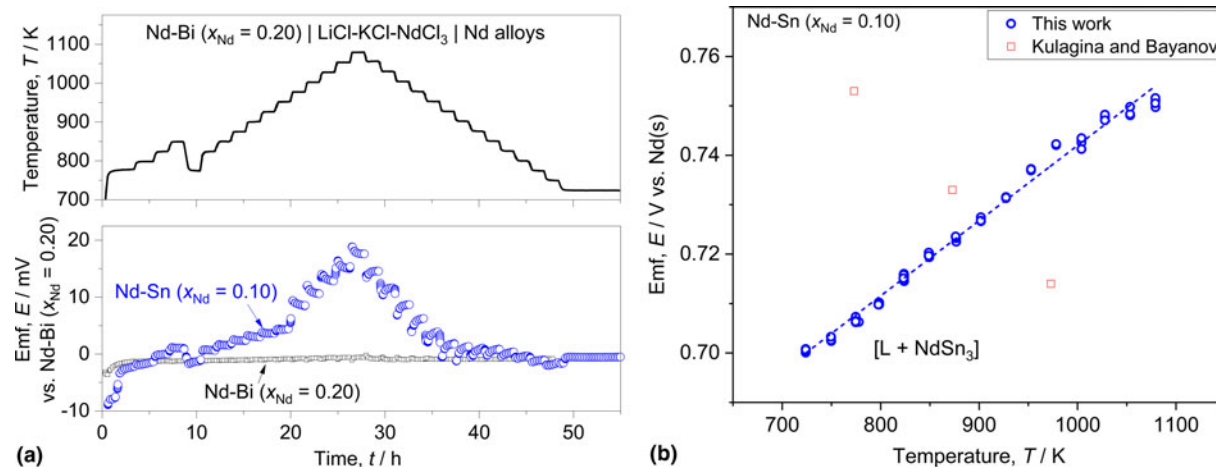


Figure 6: (a) Emf measurements of Nd-Sn ($x_{Nd} = 0.10$) during the thermal cycle using Nd-Bi ($x_{Nd} = 0.20$) as the RE in the molten LiCl-KCl-NdCl₃ electrolyte and (b) emf of Nd-Sn ($x_{Nd} = 0.10$) as a function of temperature and the results by Kulagina and Bayanov [15], where the dashed line represents a linear fit.

and, thus, continuously decreases the emf of the Nd-Sn alloy, as observed and described earlier (Fig. 1).

Thermodynamic properties of Nd alloys

Based upon the emf-T data of Nd alloys, the change in partial molar entropy ($\Delta\bar{S}_{Nd}$) and enthalpy ($\Delta\bar{H}_{Nd}$) was calculated using the Nernst and Gibbs-Helmholtz equation:

$$\Delta\bar{S}_{Nd} = -\left(\frac{\partial\Delta\bar{G}_{Nd}}{\partial T}\right)_p = 3F\left(\frac{\partial E}{\partial T}\right)_p, \quad (8)$$

$$\begin{aligned} \Delta\bar{H}_{Nd} &= -T^2\left(\frac{\partial(\Delta\bar{G}_{Nd}/T)}{\partial T}\right)_p = 3FT^2\left(\frac{\partial(E/T)}{\partial T}\right)_p \\ &= -3F\left(\frac{\partial(E/T)}{\partial(1/T)}\right)_p. \end{aligned} \quad (9)$$

From linear fits of emf-T data [dashed lines in Fig. 5(b) and Fig. 6(b)], $\Delta\bar{S}_{Nd}$ and $\Delta\bar{H}_{Nd}$ were estimated from the slope [Eq. (8)] and the intercept at 0 K [Eq. (9)], summarized in Table 1.

Conclusions

The use of pure Nd in molten salt electrolytes (LiCl-KCl-NdCl₃ and LiF-CaF₂-NdF₃) resulted in a rapid degradation of electrochemical cells and a large uncertainty in emf measurements of Nd-Bi ($x_{Nd} = 0.20$). In this work, reliable emf measurements of Nd-Bi ($x_{Nd} = 0.20$) were achieved using (1) a solid CaF₂-NdF₃ electrolyte and (2) a transient technique of electrodepositing a small quantity of pure Nd in the molten LiCl-KCl-NdCl₃ electrolyte. The peritectic transition (L + NdBi = NdBi₂) was observed during the emf measurement as

TABLE 1: Changes in partial molar entropy ($\Delta\bar{S}_{\text{Nd}}$) and enthalpy ($\Delta\bar{H}_{\text{Nd}}$) of Nd in Nd–Bi and Nd–Sn alloys, calculated from linear fits of emf data (E versus T), where $\partial E/\partial T$ and $\partial(E/T)/\partial(1/T)$ are the slope and intercept, respectively.

x_{Nd}	T (K) [phases]	$\partial E/\partial T$ ($\mu\text{V}/\text{K}$)	$\partial(E/T)/\partial(1/T)$ (mV)	$\Delta\bar{S}_{\text{Nd}}$ (J/mol K)	$\Delta\bar{H}_{\text{Nd}}$ (kJ/mol)	Adjusted R^2
Nd–Bi alloy						
0.20 ^a	760–912 [L + NdBi ₂]	141 (± 12)	606 (± 9)	41 (± 4)	–175 (± 3)	0.85
0.20 ^a	912–1035 [L + NdBi]	–48 (± 15)	777 (± 15)	–14 (± 4)	–225 (± 5)	0.34
0.40	773–912 [NdBi ₂ + NdBi]	201 (± 8)	551 (± 7)	58 (± 3)	–159 (± 2)	0.98
Nd–Sn alloy						
0.10	724–1075 [L + NdSn ₃]	152 (± 1)	590 (± 3)	44 (± 1)	–171 (± 2)	0.99

^aLinear fit was estimated using the emf data from the solid CaF₂–NdF₃ electrolyte [Fig. 5(b)]. The standard errors in the parentheses represent the 95% confidence interval of the fit.

the discontinuity in the slope (dE/dT), in agreement with the DSC measurement.

The Nd–Bi ($x_{\text{Nd}} = 0.20$) alloys were employed as a stable reference electrode in the molten LiCl–KCl–NdCl₃ electrolyte, utilizing the two-phase behavior and reduced reactivity compared to pure Nd(s). The measured emf values of Nd–Bi ($x_{\text{Nd}} = 0.15$ –0.40) and Nd–Sn ($x_{\text{Nd}} = 0.10$) were stable and reproducible without an indication of cell degradation during the measurements. Using the temperature-dependent emf data, the thermodynamic properties of Nd alloys were determined, including the activity and the partial molar quantities of Gibbs energy, entropy, and enthalpy. The methodologies established in this work would enable reliable thermodynamic property measurements of energy-critical rare-earth materials.

Materials and Methods

Fabrication of electrochemical cell components

Molten salt electrolytes

Two types of molten salts, LiCl–KCl–NdCl₃ (58.6–40.4–1.0 mol%) and LiF–CaF₂–NdF₃ (20.6–78.4–1.0 mol%), were prepared from appropriate weights of pure salts: LiCl (anhydrous, 99.9%, Alfa Aesar), KCl (anhydrous, 99.95%, Alfa Aesar), NdCl₃ (anhydrous, 99.5%, Alfa Aesar), LiF (99.99%, Alfa Aesar, Stock No. 10736), CaF₂ (99.5%, Alfa Aesar, Stock No. 11055), and NdF₃ (anhydrous 99.9%, Strem Chemical, Stock No. 93-6023) powders.

The LiCl–KCl–NdCl₃ mixture was loaded into a quartz crucible (Technical Glass Products) for premelting in a stainless-steel vacuum chamber. The chamber was loaded in a crucible furnace (Mellen, CC-12), evacuated to ~ 1 Pa, and heated in a vacuum at 373 K for 12 h and at 543 K for 12 h to remove residual moisture and oxygen. The chamber was then purged with ultra-high purity Ar three times and heated at 973 K for 3 h to premelt the electrolyte under a slow-flowing Ar (50 mL/min). After cooling, the dry and homogeneous electrolyte was ground into a fine powder using a mortar and pestle for use in the electrochemical cell.

Similar procedures were employed in preparing the LiF–CaF₂–NdF₃ electrolyte, with the exception of the premelting temperature at 1123 K due to its higher melting point and the use of a graphite crucible (Graphite store, Stock No. GT001647) to prevent the dissolution of oxides in molten fluorides.

Solid CaF₂–NdF₃ electrolyte

Binary CaF₂–NdF₃ (97–3 mol%) electrolyte was prepared by mixing appropriate amounts of NdF₃ and CaF₂ powders. Approximately 500 g of the binary mixture was added with 40 g of polyvinyl alcohol as a binder and 1 L of isopropyl alcohol as a suspension medium. The mixture was ball-milled using yttria-stabilized zirconia media (3 mm diameter, TOSO USA) for 24 h and then air-dried. About 130 g of the ball-milled, dry powder was uniaxially pressed at 30 MPa into a green pellet (75 mm diameter and 17 mm thickness). Seven wells (each with 11.2 mm diameter and 12 mm depth) were drilled into the pellet: one in the center for a thermocouple and six wells for pure Nd and Nd alloys, evenly spaced about 25.4 mm from the center. The pellet was heated in a box furnace at 393 K for 12 h to remove moisture, at 823 K for 12 h to burn out the organic binder, and at 1273 K for 3 h to sinter. Powder X-ray diffraction (XRD; PANalytical Empyrean) measurements on the sintered CaF₂–NdF₃ electrolyte confirmed the formation of a single-phase solid solution with a fluorite structure (Fig. 7) [28]. Similarly, electrolyte caps were fabricated and sintered from ~ 4 g of the mixture (19 mm diameter and 10 mm height) with a 1 mm center hole. During the final cell assembly, these caps were placed on top of the wells to minimize cross-contamination between electrodes through vapor-phase transport at elevated temperatures.

Nd alloy electrodes

The Nd–Bi ($x_{\text{Nd}} = 0.10$ –0.40) and Nd–Sn ($x_{\text{Nd}} = 0.10$) alloys were fabricated using a laboratory arc-melter (MAM-1, Edmund Bühler GmbH) under an inert Ar atmosphere from pure metals of Nd (99.1%, Alfa Aesar, Stock No. 00214), Sn (99.9999%, Alfa Aesar, Stock No. 45481), and Bi (99.9999%,

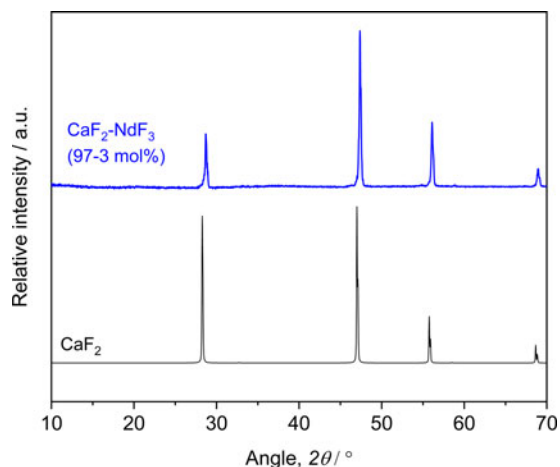


Figure 7: XRD pattern of the sintered $\text{CaF}_2\text{-NdF}_3$ (97–3 mol%) electrolyte, compared to the patterns of pure CaF_2 (fluorite) [28].

Sigma-Aldrich, Stock No. 556130). Each alloy was arc-melted at least 3–4 times to ensure a homogeneous composition.

Thermal analysis

DSC measurement was conducted using a thermal analyzer (Netzsch, STA 449 F3 Jupiter) for the Nd–Bi alloy ($x_{\text{Nd}} = 0.20$) at 20 K/min under high purity Ar flow. Approximately 20–50 mg of the alloy was placed in an alumina sample crucible with a tungsten foil interlayer to prevent direct reaction between the Nd alloy and the alumina. The phase transition temperatures were determined from the onset temperatures for characteristic transitions during the heating cycle [29].

Electrochemical cell assembly and emf measurements

Assembly of all electrochemical cells was conducted in an Ar-filled glovebox ($\text{O}_2 < 0.5$ ppm) due to the hygroscopic nature of halide salts and the reactivity of Nd alloys in an

ambient atmosphere. In each cell, two REs of the same composition (pure Nd or Nd–Bi at $x_{\text{Nd}} = 0.20$) were included to monitor the stability of the RE during the measurements. The assembled cell was placed in a stainless-steel test chamber. The chamber was sealed, removed from the glovebox, loaded into a crucible furnace, and evacuated to ~ 1 Pa. The test chamber was heated at 373 K for 12 h and at 543 K for 12 h to remove residual oxygen and moisture; purged three times with ultra-high purity Ar; and heated to a specific temperature under flowing Ar (~ 10 mL/min). The detailed procedures of cell assembly and operation are given in the following sections for each electrolyte system.

The cell emf (E), the potential difference between the WE and the RE, was measured using a potentiostat-galvanostat (Autolab PGSTAT302N, Metrohm AG) during thermal cycles in 25 K increments at a rate of ± 5 K/min. The cell temperature was held constant at each increment for ~ 1.5 h to reach thermal and electrochemical equilibria. The cell temperature was measured using a thermocouple (ASTM type-K) located at the center of the electrochemical cell and thermocouple data acquisition system (NI 9211, National Instruments).

Molten salt electrolytes

The homogeneous Nd alloys were re-melted inside boron nitride (BN; Saint-Gobain Advanced Ceramics, Product No. AX05) crucibles (12 mm outer diameter, 8 mm inner diameter, 35 mm height, and 30 mm depth), using an induction heater (IH15A-2T, Across International) custom-installed inside the glove box. The contact between the Nd alloy and the electrolyte was established through two holes (1 mm diameter) drilled through the BN walls at 7 mm from the bottom of the crucible. A tungsten or molybdenum wire (1 mm diameter, 46 cm length) was inserted into the alloy during the melting process as an electrical lead, sheathed with an alumina tube for electrical insulation with the stainless-steel flange, and sealed with epoxy at the top. Alloy electrodes and thermocouple were

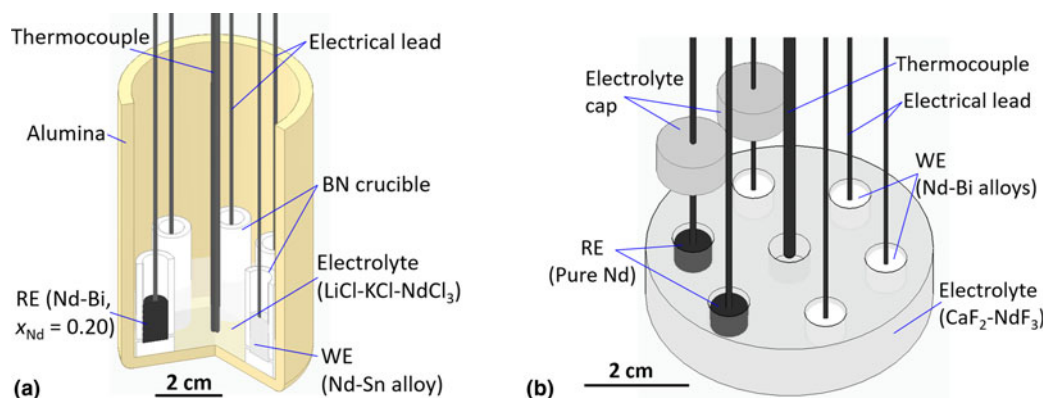


Figure 8: Schematics of electrochemical cells for emf measurements using (a) a molten LiCl-KCl-NdCl_3 electrolyte and (b) a solid $\text{CaF}_2\text{-NdF}_3$ electrolyte.

arranged in inside a crucible, and approximately 80 g of the electrolyte was poured over the electrodes.

For LiCl–KCl–NdCl₃, the electrochemical cell [Fig. 8(a)] was contained in an alumina crucible (60 mm diameter, 100 mm height, Advalue Technology), heated to 700 K, and thermally cycled between 700 and 1000 K. For molten LiF–CaF₂–NdF₃, the cell was assembled in a graphite crucible (64 mm diameter, 95 mm height; Graphite store), heated to 1050 K, and thermally cycled between 1050 and 1250 K.

Solid CaF₂–NdF₃ electrolyte

The arc-melted Nd and Nd–Bi alloys were machined into cylindrical shapes (10 mm diameter and 7 mm height) with a 2 mm center hole to insert a tungsten electrical lead during cell assembly. Six electrodes were loaded in six wells in the electrolyte; the electrolyte was placed in an alumina crucible (8.2 cm diameter, 3.0 cm height); and the tungsten wires (1 mm diameter) were inserted through the electrolyte caps and into the electrodes. A thicker tungsten electrical lead (1.5 mm diameter) was used for pure Nd metal to apply mechanical pressure to improve mechanical contact between the Nd metal and the electrolyte. The cell [Fig. 8(b)] with the CaF₂–NdF₃ electrolyte was heated to 1025 K to establish electrical contact with the Nd–Bi alloy electrodes and thermally cycled between 750 and 1025 K.

Three-electrode cell in LiCl–KCl–NdCl₃ (transient emf measurements)

The three-electrode cell was comprised of W wire (1 mm diameter) as the WE, two-phase Nd–Bi ($x_{\text{Nd}} = 0.20$) alloy as the RE, and liquid Nd–Bi ($x_{\text{Nd}} = 0.02$) as the counter electrode (CE). The two-phase Nd–Bi RE was fabricated in the BN crucible using the procedure described above. The liquid CE was fabricated by induction melting 18 g of Bi in a BN crucible (25 mm outer diameter, 22 mm inner diameter, 15 mm height, and 11 mm depth), followed by a gradual addition of Nd pieces to the target composition ($x_{\text{Nd}} = 0.02$).

The electrodes and thermocouple were arranged in an alumina crucible, and ~80 g of the LiCl–KCl–NdCl₃ electrolyte was poured into the crucible. The cell was initially heated to 800 K and gradually increased up to 1050 K. In each increment, the cell was equilibrated for 3 h prior to electrochemical measurements.

Acknowledgments

This work was supported by the US National Science Foundation (Grant No. CBET-1844170), the US Department of Energy, Office of Nuclear Energy's Nuclear Energy University Programs (Award No. DE-NE0008757), and

Integrated University Program Graduate Fellowship (Award No. DE-NE0000113).

Conflict of interest

There are no conflicts to declare.

Author Contributions

The manuscript was written through contributions of all authors. All authors have given approval to the final version of the manuscript.

Funding

This work was funded by the US National Science Foundation and the US Department of Energy, Office of Nuclear Energy.

References

1. U.S. Department of Energy, Critical Materials Strategy, DOE/PI-0009 (2011).
2. J.L. Romero and S.A. McCord: *Rare Earth Elements: Procurement, Application, and Reclamation*. Report number SAND2012-6316 (2012).
3. J.G. Price: Energy critical elements: Securing materials for emerging technologies. *Miner. Eng.* **63**, 33 (2011).
4. M.S. Foster, S.E. Wood, and C.E. Crouthamel: Thermodynamics of binary alloys. I. The lithium-bismuth system. *Inorg. Chem.* **3**, 1428 (1964).
5. W. Weppner and R.A. Huggins: Thermodynamic properties of the intermetallic systems lithium-antimony and lithium-bismuth. *J. Electrochem. Soc.* **125**, 7 (1976).
6. T. Yih and J.C. Thompson: Chemical potentials and related thermodynamic properties of molten Na–Cs and Na–Bi alloys. *J. Phys. F Met. Phys.* **12**, 1625 (1982).
7. H. Kim, D.A. Boysen, D.J. Bradwell, B. Chung, K. Jiang, A.A. Tomaszowska, K. Wang, W. Wei, and D.R. Sadoway: Thermodynamic properties of calcium-bismuth alloys determined by emf measurements. *Electrochim. Acta* **60**, 154 (2012).
8. T. Lichtenstein, N.D. Smith, J. Gesualdi, K. Kumar, and H. Kim: Thermodynamic properties of barium-bismuth alloys determined by emf measurements. *Electrochim. Acta* **228**, 628 (2017).
9. N.D. Smith, T. Lichtenstein, J. Gesualdi, K. Kumar, and H. Kim: Thermodynamic properties of strontium-bismuth alloys determined by electromotive force measurements. *Electrochim. Acta* **225**, 584 (2017).
10. K. Liu, Y.L. Liu, Z.F. Chai, and W.Q. Shi: Evaluation of the electroextractions of Ce and Nd from LiCl–KCl molten salt using liquid Ga electrode. *J. Electrochem. Soc.* **164**, D169 (2017).

11. **P. Masset, R.J.M. Konings, R. Malmbeck, J. Serp, and J.P. Glatz:** Thermochemical properties of lanthanides (Ln = La, Nd) and actinides (An = U, Np, Pu, Am) in the molten LiCl-KCl eutectic. *J. Nucl. Mater.* **344**, 173 (2005).
12. **H. Hayashi, M. Akabori, T. Ogawa, and K. Minato:** Spectrophotometric study of Nd²⁺ ions in LiCl-KCl eutectic melt. *Z. Naturforsch. A* **59**, 705 (2004).
13. **A. Novoselova and V. Smolenski:** Electrochemical behavior of neodymium compounds in molten chlorides. *Electrochim. Acta* **87**, 657 (2013).
14. **V.A. Lebedev, V.I. Kober, and L.F. Yamshchikov:** *Thermochemistry of Rare-Earth Metals and Actinide Elements Alloys* (Metallurgiya, Chelabinsk, 1989).
15. **N.G. Kulagima and A.P. Bayanov:** An electromotive force study of the thermodynamic properties of neodymium trisulfide and its solutions in liquid tin. *Russ. J. Phys. Chem.* **48**, 273 (1974).
16. **V.A. Lebedev and C.C. Akhmedov:** Thermodynamic properties of solid and liquid neodymium-magnesium alloys. *Russ. Metall.* **2011**, 133 (2011).
17. **C. Hamel, P. Chamelot, and P. Taxil:** Neodymium(III) cathodic processes in molten fluorides. *Electrochim. Acta* **49**, 4467 (2004).
18. **T. Lichtenstein, J. Gesualdi, T.P. Nigl, C.T. Yu, and H. Kim:** Thermodynamic properties of barium-antimony alloys determined by emf measurements. *Electrochim. Acta* **251**, 203 (2017).
19. **T.P. Nigl, T. Lichtenstein, N.D. Smith, J. Gesualdi, Y. Kong, and H. Kim:** Thermodynamic properties of strontium-lead alloys determined by electromotive force measurements. *J. Electrochem. Soc.* **165**, H991 (2018).
20. **N.D. Smith, N. Orabona, T. Lichtenstein, J. Gesualdi, T.P. Nigl, and H. Kim:** Thermodynamic properties of Sr-Sb alloys via emf measurements using solid CaF₂-SrF₂ electrolyte. *Electrochim. Acta* **305**, 547 (2019).
21. **C.P. Wang, H.L. Zhang, A.T. Tang, F.S. Pan, and X.J. Liu:** Thermodynamic assessments of the Bi-Nd and Bi-Tm systems. *J. Alloys Compd.* **502**, 43 (2010).
22. **A. Ovchinnikov, J.P.A. Makongo, and S. Bobev:** Yet again, new compounds found in systems with known binary phase diagrams. Synthesis, crystal and electronic structure of Nd₃Bi₇ and Sm₃Bi₇. *Chem. Commun.* **54**, 7089 (2018).
23. **R.A. Sharma and R.N. Seefurth:** Thermodynamic properties of the lithium-silicon system. *J. Electrochem. Soc.* **123**, 1763 (1976).
24. **S. Poizeau, H. Kim, J.M. Newhouse, B.L. Spatocco, and D.R. Sadoway:** Determination and modeling of the thermodynamic properties of liquid calcium-antimony alloys. *Electrochim. Acta* **76**, 8 (2012).
25. **J.M. Newhouse, S. Poizeau, H. Kim, B.L. Spatocco, and D.R. Sadoway:** Thermodynamic properties of calcium-magnesium alloys determined by emf measurements. *Electrochim. Acta* **91**, 293 (2013).
26. **M.M. Kane, J.M. Newhouse, and D.R. Sadoway:** Electrochemical determination of the thermodynamic properties of lithium-antimony alloys. *J. Electrochem. Soc.* **162**, A421 (2015).
27. **J. Kim, E. Thibodeau, K. Tetley-Gerard, and I.H. Jung:** Critical evaluation and thermodynamic optimization of the Sn-RE systems: Part I. Sn-RE system (RE = La, Ce, Pr, Nd and Sm). *Calphad* **55**, 113 (2016).
28. **R.T. Downs and M. Wallace-Hall:** The American mineralogist crystal structure database. *Am. Mineral.* **88**, 247 (2003).
29. **W.J. Boettinger, U.R. Kattner, K-W. Moon, and J.H. Perepezko:** DTA and Heat-Flux DSC Measurements of Alloy Melting and Freezing, NIST, Special Publication 960-15 (2006).